STM AND AFM INVESTIGATION OF CARBON NANOTUBES

L. P. Biró[1, 2], G. I. Márk[1], J. Gyulai[1], P. A. Thiry[2]

[1]MTA-Research Institute for Technical Physics and Materials Science, H-1525 Budapest, P. O. Box 49, Hungary

[2]Facultés Universitaires Notre Dame de La Paix, LASMOS, Rue de Bruxelles 61 , B-5000, Namur Belgium

e-mail: biro@mfa.kfki.hu

Carbon nanotubes are a new allotrope of carbon which emerged from the fullerene family [1]. Carbon nanotubes have been discovered by high resolution transmission electron microscopy (HRTEM) in 1991 by Iijima [2]. A single wall carbon nanotube is constituted of one atomic plane with a graphite-like arrangement of C atoms – called a graphene sheet – which is perfectly rolled into a cylinder (Fig. 1). Typical tube diameters are in the nm range. The multi-wall carbon nanotubes are built from several coaxial layers of graphene cylinders with an interlayer spacing of 3.4 E. Their external diameters are in the range of several tens of nm. The ends of a carbon nanotube may be capped by a fullerene-like (a higher fullerene-like hemisphere), or the tube end may be open.

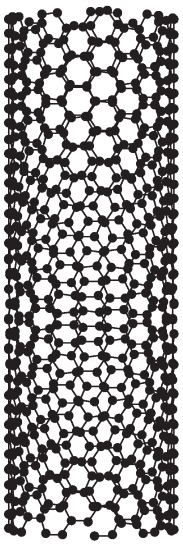

Fig. 1

Fig. 1. Stick and ball model of a chiral (9,11) single wall carbon nanotube.

Carbon nanotubes have remarkable electronic and mechanical properties which let them be in the focus of the research in recent years. They may have metallic or semiconducting behaviour depending on the way the graphene sheet is rolled to form the tube. The most important theoretical and experimental results have been summarized in Ref. [3], and Ref. [4]. Recent reports showed that there is good agreement between theoretically predicted gap values and experimental measurements on single wall carbon nanotubes [5]. Experimental results point to the possibility of building nanometer- sized electronic devices based on carbon nanotubes [6, 7]. The first working flat panel display based on carbon nanotube field emitters has been reported recently [8]. To make possible technological applications of carbon nanotubes, characterization tools have to be found, which are able to probe the physical and mechanical properties of *individual* nanotubes. Scanning tunnelling microscopy (STM), and atomic force microscopy (AFM) are uniquely suited for the investigation of nano-objects with typical dimensions in the nm range. These techniques have been successfully used for the geometric characterization of carbon nanotubes, and for acquiring data about the electronic, electric and mechanical properties of *individual* carbon nanotubes.

The first atomic resolution STM image of a carbon nanotube was reported by Ge and Sattler [9]. The STM images showed the same atomic periodicity as for highly oriented pyrolytic graphite (HOPG). The next important step was the first scanning tunnelling spectroscopy (STS) measurements done by Olk and Heremans [10]. These authors conclusively showed that indeed there are nanotubes which exhibit semiconductor like behaviour. However, their experimental gap values showed a diameter dependent deviation from the theoretically predicted linear dependence on the reciprocal diameter of the tube. This may be an indication that the experimentally measured diameter values were distorted. Recently Zettl [6] and coworkers using the STM tip as a sliding contact showed that along the axis of a nanotube there are regions with ohmic behaviour and other ones which exhibit a strong rectification. Most recently two independent groups achieved low temperature STM measurements and showed simultaneously atomic resolution STM imaging with STS measurements [5]. While the data of Lieber and coworkers show a diameter independent deviation from the theoretical behavior, the data reported by Dekker and coworkers show a diameter dependent deviation. In both cases these deviations are significantly smaller than in the early work of Olk and Heremans. Our earlier work on the STM image formation mechanism during the imaging of carbon nanotubes in constant current mode showed that the apparent diameter of a carbon nanotube in the STM image depends on several factors which cannot be neglected [11, 12], recent computer simulation results gave more insight in the intrinsic mechanism of image formation [13].

The way in which the STM image of a carbon nanotube is formed is influenced by two major factors: i) the differences between the electronic properties of the nanotube itself, and of the substrate on which it is deposited; and ii) the geometric characteristics of the apex of the STM tip. In some favourable cases it is possible to get an experimental

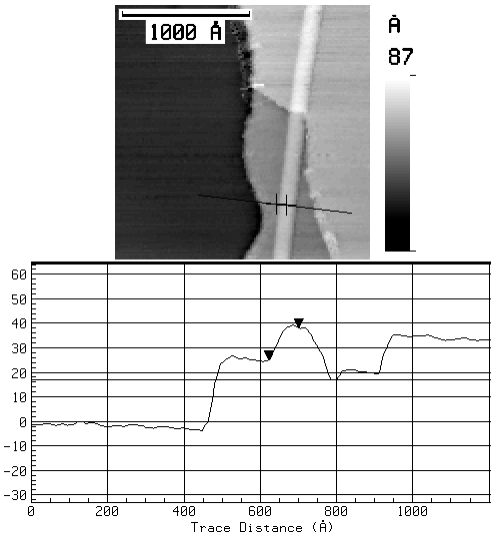

Fig. 2 Constant current STM image of a carbon nanotube on HOPG in an area with two cleavage steps, $U_t = 0.1$ V, $I_t = 0.85$ nA, scan rate 1 Hz. The line cut below the image is taken along the black line marked in the image, marker positions seen in the line cut are identified by crosses in the image.

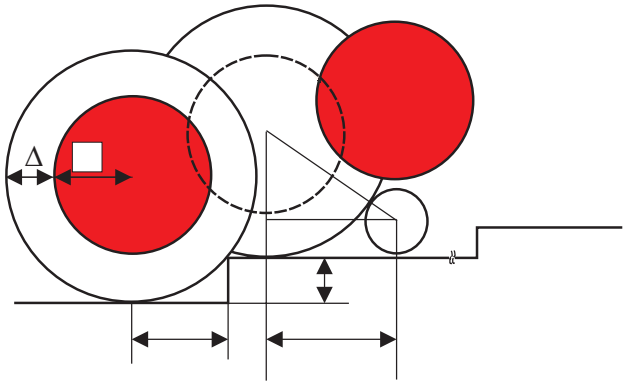

Fig. 3. Schematic topography and selected tip positions from Fig. 2. The geometrical tip is shown by the shaded circle, while the outer circle, of radius $R + \Delta$, shows the effective tip. Position I: the tip comes into "tunneling contact" with the first step. Position II: the tip comes into tunneling contact with the nanotube. Position III: the tip over the topmost point of the nanotube, note the reduced separation between tip and sample as compared with position I. The carbon nanotube – light circle at B – is not touching the substrate, it floats at a distance of 3.4 Å over the HOPG substrate.

insight in the way these factors influence the image formation. In Fig. 2 the image of a carbon nanotube crossing two cleavage steps on HOPG is shown. Taking a line cut across the steps and the nanotube, and using the procedure given in [14] one can obtain the effective tip radius $R_{eff} = R + \Delta$ from the rounding observed at the step edges (see position *I* in Fig. 3). Using R_{eff} one can calculate from the apparent half width (HW) of the tube, the geometric tube radius (see position II in Fig. 3). For the case shown in Fig. 2, with an average $R_{eff} = 72$ E (all dimensions are averaged over 5 independent measurements; R_{eff} has been determined independently on the two cleavage steps visible in the image), using a simple geometric model of a cylindrical object of radius r floating at the distance $\delta = 3.4$ Å above a flat surface, which is scanned by a tip with radiu R_{eff}, one may calculate the geometric tube radius, $r = 18$ Å. This number, if compared with the measured half diameter, *HW*, of 77 Å, shows that the apparent diameter of the tube will be 4 times its geometric diameter. In agreement with results reported earlier [11], the measured tube height $h_m = 15$ Å is significantly smaller than the value which results from pure geometric considerations $h_g = 2r + \delta = 39.4$ Å. The causes of the difference are twofold. First, the very large R_{eff} makes that a spherical cap of about 12 Å in radius has to be considered as being within the distance $d = \Delta + 1$Å of the flat substrate surface, and thus, should be considered as giving contribution to the tunnelling current. This will make that the value of Δ will be larger than for an ideal, single atom tip. Second, due to the low tunneling trans- conductance through the nanotube as compared with the substrate - arising from the difference of electronic structures of the substrate and of the nanotube, and from the existence of two tunnelling gaps - the tip, after coming into position *II* in Fig. 3, will not follow the real geometric profile of the nanotube, but will pass over the tube at a smaller separation than Δ (position *III*), or may even touch the nanotube. These distortion effects arise from the way the tunnelling takes place through a system of two gaps [13]**.** In Fig. 4 a selection is shown from the detailed simulation of the tunnelling process. One may note that in the three snapshots shown, the evolution of tunnelling strongly depends on the particular tip position along the horizontal axis. Detailed simulations showed [13] that even in the case of identical electronic structure and identical radii, $R = r$, a purely geometric convolution will yield an apparent diameter 2.7 times the geometric diameter of the nanotube. The differ-

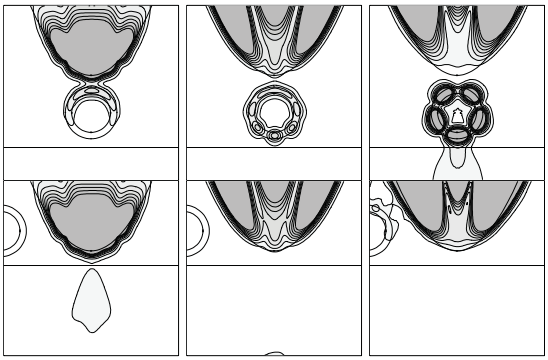

Fig. 4. Simulation by the numerical solving of the time dependent Schrödinger equation for tunneling through an STM tip - carbon nanotube - substrate system. The charge is launched from the tip towards the carbon nanotube shown as a double cylinder floating over the flat substrate. The different charge density distribution at selected time instants are displayed horizontally, while the two rows correspond to two tip positions: upper row, the STM tip is right over the topmost point of the nanotube; lower row: the STM tip is a lateral distance from the nanotube at which the tunnelling takes place dominantly directly into the substrate.

ence in the electronic structures can be taken into account in the first approximation as a modification of the width of the gap which separates the STM tip from the point to which the tunnelling takes place. This is illustrated in position III of Fig. 3. In constant current imaging the feedback loop will push the tip closer if the tunnelling current decreases, or will pull it away from the sample if the current increases. When the tip is placed right over the nanotube, if the overall tunnelling probability through the two gaps and the nanotube is smaller than the one corresponding to the substrate, the tube will appear flattened due to the approach of the STM tip until the same tunnelling current is measured as over the substrate. Under certain circumstances, the occurrence of point-contact imaging [15] in the topmost regions of the nanotube can not be excluded. In this case, mechanical deformations of the nanotube under the pressure of the STM tip can take place. Indeed, when imaging the nanotube shown in Fig. 2 at the higher tunnelling current of 1 nA, in some images a small dip appeared in the topmost part of the tube, more clearly than in the line cut shown in Fig. 2. The measured average width of this dip was 26 E, while its depth was 0.4 E. It indicates that indeed,

Fig. 5. Atomic resolution image taken in the topmost region of the same carbon nanotube as shown in Fig. 2, $U_b = 0.1$ V, $I_t = 1.0$ nA, scan rate 3 Hz: a) topographic image displaying the three axes along which the tunneling current maxima are found; b) line cut along direction AB showing the atomic corrugation amplitude and the periodicity of 2.57 E.

the tip comes into "mechanical" contact with the nanotube.

The ratio HW/h_m shows only little variation with the value of the tunneling current. For the nanotube shown in Fig. 2, imaged at a bias of 0.1 V and for the tunnelling current of 0.85 nA this ratio is 5.06, while at the same bias, but at the current of 1 nA, when the dip was observed, the ratio is 5.31. So, the apparent deformation of the nanotube is mainly a function of the tip shape and of the difference between the electronic structures of the substrate and of the nanotube.

Atomic resolution images of the same nanotube, Fig. 5, allowed the determination of its chiral angle, 12°. This, together with its calculated geometric radius of 18 E, indicates a (39.11) tube, with a calculated chirality of 12.08° and a calculated diameter of 35.62 E. The amplitude of the atomic corrugation, as seen from the line cut, is 0.5 E, about half the usual value for highly oriented pyrolytic graphite under similar experimental conditions. The periodicity of the maxima as given by Fourier analysis is 2.57 E in good agreement with the 2.45 E value for HOPG. Both, the value of the tube radius and this periodicity indicate a multi-wall carbon nanotube.

Fig. 6. Tapping mode AFM image of a sputtering crater on graphite irradiated with 209 MeV Kr ions. Two carbon nanotubes labeled by A and B emerge from the crater.

AFM, like STM proved to be a very useful technique for the investigation of carbon nanotubes. However, the early work of Höpfer et al. [16] already showed that the convolution of tip shape with the tube shape has a significant influence on the AFM image of a carbon nanotube. AFM measurements with a conductive tip were successfully used to measure the electrical transport properties of carbon nanotubes [17]. Carbon nanotubes themselves, were used as long, very thin and flexible TM AFM probes [18]. It is possible to use carbon nanotubes as AFM probes due to their exceptionally high Young modulus of the order of 1 GPa as determined from AFM measurements [19]. However, when adsorbed on the surface of the support, carbon nanotubes may suffer remnant bending [20].

In a recent report [21] we showed that carbon nanotube growth may take place on the surface of graphite targets irradiated with high energy (E > 100 MeV), heavy ions. Those dense nuclear cascades – produced in higher order collisions and being directed from the bulk to surface – which cross the surface of a graphite target will produce extensive sputtering. Nanotubes may start growing in the expanding cloud formed by sputtered target atoms and clusters. After the first, fast growth stage, the already formed carbon nanotube collapses onto the surface of the target, where additional growth takes place by the incorporation of diffusing C atoms, which were displaced from lattice positions, but do not have enough energy to leave the target surface. In Fig. 6 the tapping mode (TM) AFM image of a surface crater of 1 μm in diameter with a depth of

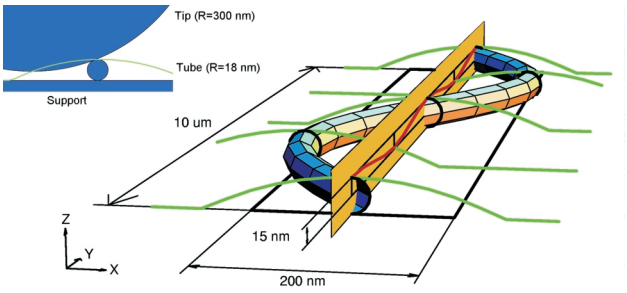

Fig. 7. Three dimensional detail of the bottom of the crater shown in Fig. 6. Two short nanotubes are shown, which cross each other close to the right hand lower corner of the image. Note the undulating profile of the nanotube situated closer to the observer.

Fig. 8. Schematic drawing showing the mechanism which is responsible for the undulation seen in Fig. 7. The nanotube oscillates in the horizontal plane (XY), parallel to the equilibrium position marked by the vertical plane (parallel with ZY), *this oscillation is not shown in the image*. The oscillation makes that in consecutive scans the AFM probe encounters the nanotube in positions which correspond to different elongation measured from the vertical plane. This will yield the "snaking" shape shown in the image. The AFM tip describes in each scan line a curve normal to the snaking form, due to the convolution of tip shape with the tube shape - see inset in the left upper corner - the nanotube will appear broadened in the curves corresponding to individual scan lines; a few selected scan lines are shown in the figure. A longitudinal line cut, or a three dimensional image, like that in Fig. 7, will show along the tube axis the undulation which results from the intersection of these curves with a vertical plane (parallel with ZY), as shown in the figure.

74 nm is shown. Two carbon nanotubes emerge from the crater, the one labeled by A, has a length exceeding 15 μm. Fig. 7 shows a three dimensional detail of the bottom of the crater seen in Fig. 6. One may note the presence of two shorter carbon nanotubes in the crater. The height, i.e., the diameter of the nanotubes emerging from the crater in Fig. 6 is 11 nm for tube A, and 10 nm for tube B, respectively, while the shorter nanotubes in the crater, have diameters in the range of 13 nm. The measured tube height is free of distortion arising from tube and tip shape convolution [16], therefore it is taken as the correct value for the diameter of the nanotube. Usually, blunt tips with radii greater than 100 nm were preferred, due to the convolution effects these tips yield an artificial „enlargement" of the nanotube in the plane of the image, facilitating in this way the finding of the nanotube in large scan windows of several thousands of μm^2.

As seen in Fig. 7, the nanotube which crosses the other one shows „undulation", while all the other topographical features of the image show a regular profile. This behavior was frequently found for those nanotubes which cross elevated surface features. The undulation is the consequence of the vibration of the carbon nanotube. A vibrating object when imaged by a probe which scans the sample with constant frequency (a scan frequency of 1 Hz was used) will yield maxima and minima as seen in Fig. 7. Fig. 8 illustrates schematically the image formation for the case of a rod like object which moves left and right parallel with the vertical plane (ZY) shown in the figure - for the immobile tube, this plane would contain the vertical diameter of the tube - with amplitude *A*, in a direction parallel with the scan direction (in plane XY). Due to the fact that the vibration frequency and the scan frequency are not equal, in consecutive scan lines the AFM tip will encounter the rod like object in positions that correspond to different elongation, therefore, the object appears as „snaking" for the AFM. This will yield a profile like that shown in the vertical plane in Fig. 8, i.e., an undulating profile [22].

In summary, STM and AFM are powerful methods for the investigation of *individual* carbon nanotubes. However, the mechanism of image formation has to be taken very carefully into account. Convolution effects arise during both STM and AFM imaging of carbon nanotubes. Furthermore, other effects like the difference of electronic properties of the carbon nanotube and of the supporting surface have to be taken in account in the interpretation of STM images, and mechanical vibration of the nanotube may not be neglected in the interpretation of AFM data.

Acknowledgments

Stimulating discussions with Prof. Ph. Lambin of FUNDP Namur are gratefully acknowledged. The authors are indebted to V. Meunier for generating the model of carbon nanotube in Fig. 1, and for helpful discussions. This work was supported in Hungary by OTKA T025928, and AKP 96/2-637 grants. L. P. Biró gratefully acknowledges a fellowship from the Belgian SSTC for S&T cooperation with Central and Eastern Europe.

References

1. H. W. Kroto, J. R. Heath, S. C. O'Brien, R. F. Curl, and R. E. Smalley, *Nature*, **318** (1985) 162.
2. S. Iijima, *Nature*, **354** (1991) 56 .
3. M. S. Dresselhaus, G. Dresselhaus, and P. C. Eklund, *Science of Fullerenes and Carbon Nanotubes*, Academic Press, San Diego, 1996.
4. Th. W. Ebbesen, Ed. Carbon Nanotubes preparation and Properties, CRC Press, Boca Raton, 1997.
5. J. W. G. Wildöer, L. C. Venema, A. G. Rinzler, R. E. Smalley & C. Dekker, *Nature*, **391**, 59 (1998); . T. W. Odom, J.-L. Huang, Ph. Kim & Ch. M. Lieber, *Nature,* **391** (1998) 62 .

6. Ph. G. Collins, A. Zettl, H. Bando, A. Thess, R. E. Smalley, *Science,* **278** (1997) 100.

7. S. J. Tans, A. R. M. Verschueren & C. Dekker, *Nature*, **393** (1998) 49.

8. Q. H. Wang, A. A. Setlur, J. M. Lauerhaas, J. Y. Dai, E. W. Seeling, and R. P. H. Chang, *Appl. Phys. Lett.*, **72** (1998) 2912.

9. M. Ge and K. Sattler, *Science*, **260** (1993) 515.

10. Ch. H. Olk and J. P. Heremans, *J. Mater. Res.*, **9** (1994) 259.

11. L. P. Biró, S. Lazarescu, Ph. Lambin, P. A. Thiry, A. Fonseca, J. B. Nagy, and A. A. Lucas, *Phys. Rev B*, **56** (1997) 12490.

12 L. P. Biró, J. B.Nagy, Ph. Lambin, S. Lazarescu, A Fonseca, P. A. Thiry and A. A. Lucas, in: *Molecular Nanostructures*, H.Kuzmany, J.Fink, M.Mehring and S.Roth (Eds.), World Scientific, Singapore 1998, p. 419.

13. G. I. Márk, L. P. Biró, J. Gyulai, *Phys. Rev. B*, **58** (1998) 12645.

14. L. P. Biró, J. Gyulai, Ph. Lambin, J. B. Nagy, S. Lazarescu, G. I. Mark, A. Fonseca, P. R. Surján, Zs. Szekeres, P. A. Thiry, and A. A. Lucas, *Carbon*, **36** (1998) 689.

15. N. Agrait, J. G. Rodrigo, S. Vieira, *Ultramicroscopy* **42** (1992) 177.

16. R. Höpfer, R. K. Workman, D. Chen, D> Sarid, T. Yadav, J. C. Withers, R. O. Loufty, *Surface Science*, **311** (1994) L731.

17. H. Dai, E. W. Wong, Ch. M. Lieber, *Science*, **272** (1996) 523.

18. H. Dai, J. H. Hafner, A. G. Rinzler, D. T. Colbert & R. E. Smalley, *Nature*, **384** (1996) 147.

19. E. W. Wong, P. E. Sheehan, Ch. M. Lieber, *Science*, **277** (1997) 1971.

20. M. R. Falvo, G. J. Clary, R. M. Taylor, V. Chi, F. P. Brooks Jr., S. Washburn & R. Superfine, *Nature*, **582** (1997) 389.

21. L. P. Biró, G. I. Márk, J. Gyulai, K. Havancsák, S. Lipp, Ch. Lehrer, L. Frey, H. Ryssel, European Materials Research Society Spring Meeteing, Symposium J, 1998, June 16 - 19, Strasbourg, France, Nucl. Instr. Meths. B, **147** (1999) 142.

22. http://www.mfa.kfki.hu/nano/pub/ecm18/index.html.